Tuning the Ground-State and Excited-State Interchromophore Interactions in Porphyrin–Fullerene π-Stacks

7 AUTHORS, INCLUDING:

Vladimir I Chukharev
Tampere University of Technology
65 PUBLICATIONS **492** CITATIONS

SEE PROFILE

Nikolai Tkachenko
Tampere University of Technology
267 PUBLICATIONS **4,607** CITATIONS

SEE PROFILE

Alexander Efimov
Tampere University of Technology
102 PUBLICATIONS **1,098** CITATIONS

SEE PROFILE

Helge Lemmetyinen
Tampere University of Technology
423 PUBLICATIONS **6,455** CITATIONS

SEE PROFILE

Tuning the Ground-State and Excited-State Interchromophore Interactions in Porphyrin–Fullerene π-Stacks

Vladimir Chukharev,*,† Nikolai V. Tkachenko,† Alexander Efimov,† Dirk M. Guldi,*,‡ Andreas Hirsch,§ Michael Scheloske,§ and Helge Lemmetyinen*,†

Institute of Materials Chemistry, Tampere University of Technology, P.O. Box 541, 33101 Tampere, Finland, Radiation Laboratory, University of Notre Dame, Notre Dame, Indiana 46556, and Institut für Organische Chemie der Universität Erlangen-Nürnberg, Henkestrasse 42, D 91054 Erlangen, Germany

Recently synthesized porphyrin–fullerene dyads with two separate linkers form a nearly symmetric complex with π-stack sandwich-like structure. The interchromophore interactions of such complexes can be fine-tuned by varying the linker lengths, which opens an opportunity to control physical and chemical properties of the dyads. Absorption spectroscopy emerged as a convenient means to register the interchromophore interactions: the spectra of the chromophores ground-state absorptions show appreciable perturbations and, more importantly, an additional absorption feature is discernible in the near-infrared region. Similarly, the emission spectra have a character typical for intramolecular exciplex. These new spectral features (i.e., absorption and emission) were attributed to a new electronic state, namely, an intramolecular preformed exciplex, featuring a common molecular orbital with a partial charge transfer (CT) character. From the mechanistic point of view, it is important that the preformed exciplex preceded the actual nonemitting charge separated (CS) state. The quantitative analysis of the CT absorption and the exciplex emission bands within the framework of the Marcus electron transfer (ET) theory allowed us to estimate the energy of the exciplex, $\Delta G°$, the solvent or outer-sphere reorganization energy, λ_s, the internal reorganization energy, λ_v, the energy of the vibrational mode, E_v, and the electronic coupling matrix element, V. Variation in the linker lengths shows that mainly the electronic coupling is affected by this structural modification, leaving the other parameters essentially unchanged. The strongest coupling, $V = 450$ cm^{-1} (0.056 eV), was observed for the dioxyethyl type of linkers, whereas in the shorter, oxymethyl type, and longer, dioxypropyl type, dyads the couplings were much weaker (190 and 270 cm^{-1}, respectively). Photodynamics of the dyads was studied in the femto- and picosecond time domains, using the emission up-conversion and absorption pump–probe techniques.

1. Introduction

Recent years have shed light onto the role of intramolecular exciplexes as one of the important intermediate steps in the photochemistry/photophysics of porphyrin–fullerene (and related) ensembles.[1–3] The exciplex intermediate has been observed as an emitting state in nonpolar media (toluene[4–6]) and in solid films.[6–8] It was also detected as a precursor to the final charge separated (CS) state in polar media.[1–3] When observed, exciplex formation exerts a strong impact on the electron transfer (ET) features of the resulting porphyrin–fullerene ensembles. Arguably its low energy might be the reason for the inability of the Zn porphyrin–fullerene dyads to undergo charge separation in nonpolar media.[1] In the exciplex the two chromophores form a common molecular orbital and its appearance depends on the mutual alignment and ordering of the corresponding porphyrin and fullerene moieties. In the most distinct exciplex manifestation, compact sandwich-like arrangements are inferred,[4,6] and it seems that this type of organization is further enforced by strong π–π interactions between the planar porphyrin and the spherical fullerene moieties.
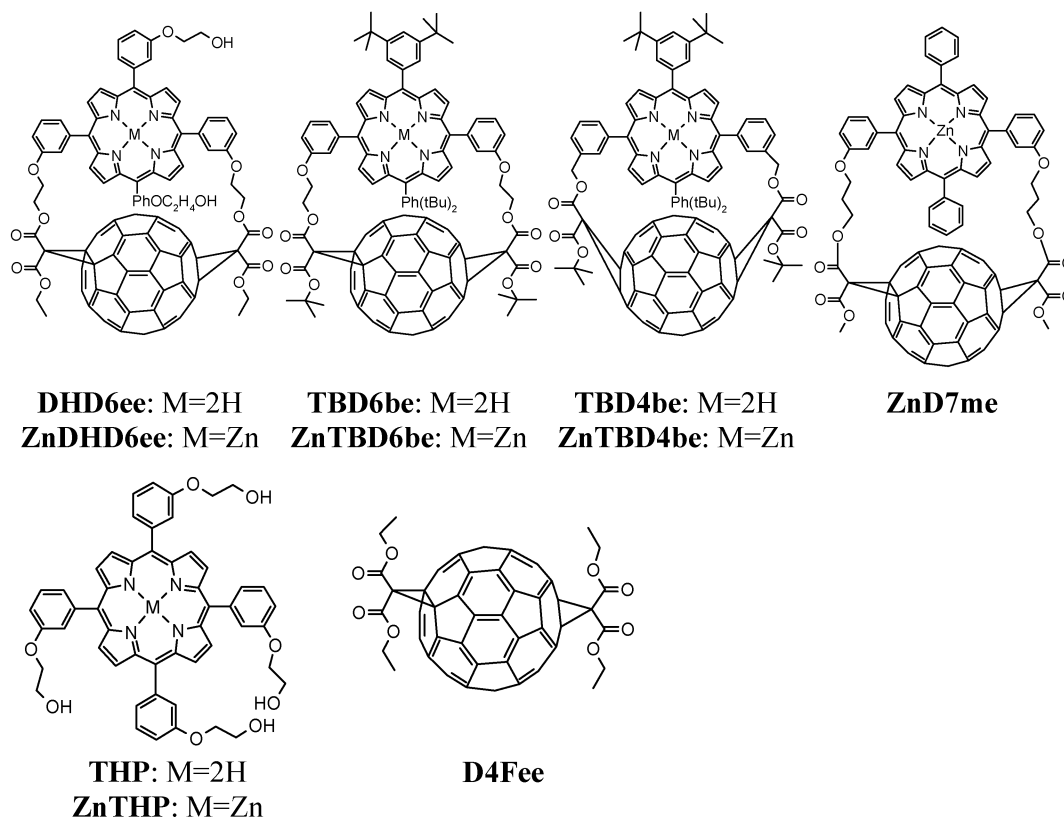
Intriguing incentives to organize porphyrin/fullerene hybrids can be borrowed from crystal structures of porphyrin/fullerene mixtures.[9] The crystal packing, found for example in the X-ray crystal structure of a fulleropyrrolidine/free base tetraphenylporphyrin hybrid,[10] gives way to a clear picture on the disposition of both moieties. An appreciable intermolecular interaction evolves from an unexpectedly close approach between C_{60} and porphyrin. The distances of the closest C_{60} C-atoms to the mean plane of the inner core of porphyrin are quite short, with values of 2.78 and 2.79 Å. This led to the formation of a new porphyrin/fullerene relationship, that is, augmentation of the usual π–π association by electron donor–electron acceptor interactions. Following the remarkable results of the initial work on a covalently linked dyad, this aspect was systematically explored in a series of porphyrin/fullerene cocrystallates, where porphyrins and fullerenes were not chemically linked to each other. Various metal species, ranging from Mn, Co, Ni, Cu, Zn to Fe, were chosen.[11] Favorable van der Waals attractions between the convex π-surface of C_{60} or C_{70} and the planar π-surface of the porphyrin assist in the supramolecular recognition, overcoming the necessity of matching a concave-shaped host with a convex-shaped guest structure. Common to all C_{60}-based cocrystallates is that electron-rich areas, i.e. carbon atoms at hexagon–hexagon junctions, lie over the center of the porphyrin ring. C_{70}, on the other hand, adapts a configuration that brings the poles of the ellipsoidal framework—again carbon atoms located at the intersection of hexagon faces—into contact with porphyrin. As a direct consequence, complexes with unusually short contacts (2.7–3.0 Å), shorter than the ordinary van der

† Tampere University of Technology.
‡ University of Notre Dame.
§ Institut für Organische Chemie der Universität Erlangen-Nürnberg.

DHD6ee: M=2H   **TBD6be**: M=2H   **TBD4be**: M=2H   **ZnD7me**
ZnDHD6ee: M=Zn   **ZnTBD6be**: M=Zn   **ZnTBD4be**: M=Zn

THP: M=2H   **D4Fee**
ZnTHP: M=Zn

Figure 1. Studied dyads and reference compounds (DH = dihydroxyl, TB = *tert*-butyl, D = double, 4, 6, 7 = number of atoms in linkers, ee = ethyl ester, me = methyl ester, P = porphyrin, F = fullerene).

Waals contacts (3.0−3.5 Å), are formed. The experimental data, such as ESR, IR, absorption, and X-ray photoelectron spectroscopy,[12] fail to indicate noticeable charge-transfer features in these porphyrin/fullerene cocrystallates, despite the porphyrins excellent electron donating ability and the electron-accepting character of C_{60}.

In recent years, attempts to model the described organization principles and to probe their impact on electron-transfer reactions led to the development of a variety of porphyrin/fullerene hybrids that give rise to different topologies and chromophore separations.[13−15] Most importantly, detailed photophysical investigations, as performed with some of these porphyrin/ fullerene hybrids, have revealed spectroscopic and kinetic evidence, which suggest that electron transfer occurs via an intramolecular exciplex.[1−3] This transient intermediate features an emission band in the near-IR region, which is, however, only detectable in nonpolar solvents. In polar solvents, on the other hand, this emission is typically not seen, or it is much weaker, due to short lifetimes and/or low formation quantum yields, but the exciplex can still be identified spectroscopically as a distinct intermediate state preceding the metastable CS state.

Most of the synthetic methodologies are based on connecting porphyrins and fullerenes by a single linker. The single linker, however, results in a substantial degree of conformational flexibility in the molecular topology and two limiting scenarios evolve: (i) the porphyrin/fullerene organization in the resulting hybrids is rather poorly defined or (ii) the fullerene cannot be brought into a position that centers on top of the porphyrinic macrocycle. A recent synthetic approach, in which porphyrins and fullerenes are brought together by two separate linkers, yields symmetrical dyads with π-stack sandwich structures.[16−19] This molecular design opens new possibilities in control over interchromophore interactions and in fine-tuning the properties of the intramolecular exciplex.

The primary goal of this study was to probe the relationship between structural effects, such as molecular organization, interchromophore distance, and choice of the coordinated metal center, and exciplex properties in a series of porphyrin/fullerene hybrids. In particular, the dyads were studied by using a wide range of steady-state and time-resolved spectroscopic techniques. As compared to other porphyrin−fullerene hybrids,[1−7,13−15] common to these π-stacked dyads is a new distinct absorption feature in the near-infrared region, which reflects an augmented electronic interaction between the two chromophores.

2. Methods and Materials

Compounds. Porphyrin−fullerene dyads involved in this study are presented in Figure 1. 61,62-Diethyl [10,20-(3-(2-hydroxyethoxy)phenyl)porphyrin-5,15-diylbis(1- phenyl-3-oxy)-diethylene] 1,9:49,59-bismethano[60]fullerene-61,61,62,62-tetracarboxylate (**DHD6ee**), 61,62-di-*tert*-butyl 61,62-[10,20-(3,5-di-*tert*-butylphenyl)porphyrin-5,15-diylbis(1-phenyl-3-oxy)diethylene] 1,9:49,59-bismethano[60]fullerene-61,61,62,62-tetracarboxylate (**TBD6be**), *out*,*out*-61,62-di-*tert*-butyl 61,62-[10,20-(3,5-di-*tert*-butylphenyl)porphyrin-5,15-diylbis(1,3-phenylene)dimethylene] 1,2:55,60-bismethano[60]fullerene-61,61,62,62-tetracarboxylate (**TBD4be**), and 5,10,15,20-tetrakis-[3-(2-hydroxyethoxy)phenyl]porphyrin (**THP**) were synthesized as described elsewhere.[18] Their zinc complexes were prepared by reaction of the free base compounds with Zn(OAc)$_2$. The synthesis and characterization of **ZnD6me** and **D5Fee** is discussed elsewhere.[20]

Spectroscopic Measurements. Absorption spectra were measured on a Shimadzu UV-2501PC spectrophotometer. Fluorescence spectra were recorded with a Fluorolog 3 (SPEX Inc.) fluorimeter equipped with a cold infrared sensitive photomultiplier (Hamamatsu R2658). The spectra were corrected by using

Tuning Porphyrin−Fullerene π-Stacks

J. Phys. Chem. B, Vol. 108, No. 42, 2004 **16379**
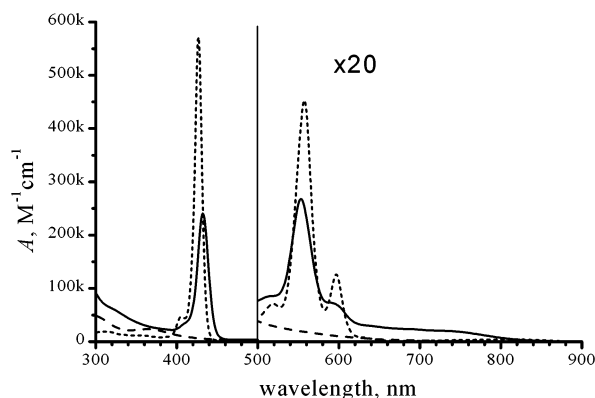
Figure 2. Absorption spectra of **ZnDHD6ee** in toluene (solid line), **ZnTHP** in toluene:methanol 25:1 (dotted line), and **D4Fee** in benzonitrile (dashed line).

a correction spectrum supplied by the manufacturer. The time-resolved fluorescence in the nanosecond time scale was measured by the time-correlated single-photon counting (TCSPC) technique. In these experiments the excitation wavelength was 590 nm, and the time resolution was about 100 ps. The fast processes were studied with a time resolution better then 0.2 ps (i.e., the instrument response time, fwhm) by means of the up conversion technique for fluorescence and the pump−probe for transient absorption measurements. Counting time in the up conversion experiments was 20 s. The excitation wavelength was 430 nm. The instruments have been described earlier.[1]

3. Results and Discussion

Most of the currently reported measurements were performed in two solvents: toluene and benzonitrile. These solvents represent nonpolar and polar environments, respectively, and their choice is expected to exert a profound impact on the interchromophore interactions, in both the ground and excited states. Introduction of the *tert*-butyl groups at the porphyrinic macrocycle enhances the overall solubility in nonpolar solvents without impacting the interactions. It allows the measurements in an even less polar solvent, namely, cyclohexane. Although we found no principal difference, when comparing the properties of the dyad in toluene with those in cyclohexane, it is notable that the spectroscopic features become much sharper in cyclohexane and are even discernible without the necessity of further manipulating the experimental data.

3.1. Absorption and Emission Spectra. Strong electronic interactions between the porphyrin and fullerene moieties in the different hybrids can be concluded from a close inspection of their absorption spectra. As an illustration the spectrum of **ZnDHD6ee** is depicted in Figure 2 together with those spectra that correspond to the reference compounds (i.e., porphyrin and fullerene). Spectral perturbations, as seen clearly for all dyads, are typical indicators for strong interchromophore interactions. In particular, the Soret band is red shifted and broadened, and its intensity is reduced. In addition, a new broad absorption is seen in the near-IR with its dominant absorption in the 650−800-nm range. The latter has previously been assigned to a charge transfer (CT) ground-state absorption,[4] where an excitation leads to the direct population of the charge separated state.

The emission spectra of the dyads in nonpolar solvents have clear exciplex features. Normalized spectra for the metal-free (**H₂P**) and zinc (**ZnP**) dyads in cyclohexane are presented in Figure 3. Besides residual porphyrin fluorescence, which is found in the 600−700-nm region, the spectra of both dyads are dominated by the exciplex-type emission with maxima at 730
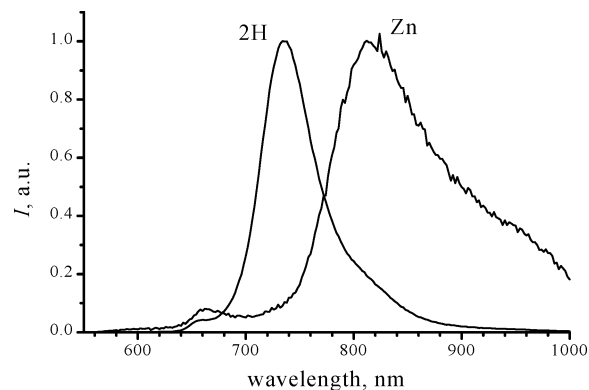
Figure 3. Normalized corrected emission spectra of **TBD6be** (2H) and **ZnTBD6be** (Zn) in cyclohexane.
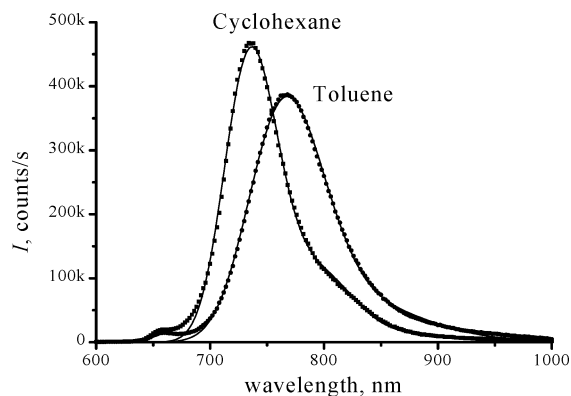
Figure 4. Emission spectra of **TBD6be** in cyclohexane and toluene. Dots are experimental points, and solid lines present fitting to eq 1.

and 810 nm, for **H₂P** and **ZnP**, respectively. This type of emission was previously detected for phytochlorin−fullerene dyads for which the ground state interaction was not spectroscopically observable in the near-IR region.[1] Importantly, the exciplex-type emission intensity decreases rapidly with an increase the solvent polarity—even a switching from cyclohexane to toluene leads to a 20% drop in the intensity—as presented in Figure 4. Additional features are a shift of the emission maximum to the red and broadening of the bandwidths in more polar solvents. These are typical measures for exciplexes.[21,22]

3.2. Interpretation of the New Absorption and Emission Features. The observed features in the ground-state absorption and emission (in the 700−850-nm region) are due to a phenomenon, which should be described in detail.

The term exciplex is, according to its definition, applied to a new interchromophoric state, which exists in the excited state only. A formal approach implies the wave function of the new excited state, Ψ'_{Ex}, which is commonly presented as the superposition of the wave functions of the locally excited states, Ψ_p of porphyrin, and Ψ_c of fullerene, $\Psi'_{Ex} = c'_p\Psi_p + c'_c\Psi_c$. In turn, consideration of the CT absorption band involves the interaction of the locally excited state with the charge transfer ground state. The state formed after the excitation in this band, commonly called as an excited CT state, is characterized by the following wave function: $\Psi''_{Ex} = c''_p\Psi_p + c''_{CT}\Psi_{CT}$, where Ψ_{CT} is the wave function of the complete charge separated (CS) state, or radical ion pair.[21,22] The relation between the coefficients c''_p and c''_{CT} can be used to evaluate the degree of the CT taking place under the excitation.[21c] If $c''_{CT} > c''_p$, the excited complex has pronounced CT character.

In the cases of both Ψ'_{Ex} and Ψ''_{Ex} the energies of the corresponding source states should be relatively close to each other

to allow the formation of the new experimentally observable state. The case of the porphyrin−fullerene systems is unique in the sense that energies of the locally excited states of both chromophores and the energy of the complete CS state are relatively close, and a reasonable consideration of the system should take into account three wave functions: $\Psi_{Ex} = c_p\Psi_p + c_c\Psi_c + c_{CT}\Psi_{CT}$. From this perspective one can talk about the mixing of the exciplex and excited CT state definitions. In the first observations[1] this state was detected as a precursor of the CS state and its main distinction was a relatively weak emission in the near-infrared region, with no detectable absorption. Therefore it was ascribed as an intramolecular exciplex. Later we observed that a strong interaction between porphyrin and fullerene results in the formation of new absorption and emission bands,[4,6,8] but no other intermediate states were observed. The emitting state was treated as an excited CT state. However, further studies[3] have demonstrated that this state is a common property of porphyrin−fullerene systems regardless of the final formation of the CS state, i.e., the exciplex Ψ'_{Ex} and the excited CT state Ψ''_{Ex} are the same state Ψ_{Ex}, which has a different degree of CT in different cases. Keeping this in mind, we will continue to call the state, denoted as Ψ_{Ex}, exciplex to distinguish it from the complete CS state (given by Ψ_{CT}).

The exciplex (or the excited CT state) can be analyzed within the framework of the Marcus electron transfer theory,[21,23] suggesting that the emission spectrum is a weighted sum of Gaussians, as follows:

$$I(v) = C_e\sum_{i=0}^{\infty}\frac{S^n}{i!}\exp\left[-\frac{(hv - \Delta G^\circ + \lambda_s + iE_v)^2}{4\lambda_s kT}\right] \quad (1)$$

where $C_e = n[(n^2 + 2)/3]^2[16\pi^2/3]v_f^3[4\pi^3/h^2\lambda_s k_B T]^{1/2}M^2 e^{-S}$, and $S = \lambda_v/E_v$.

Here, λ_s and λ_v represent the solvent/outer sphere reorganization energy and the internal reorganization energy, respectively, and ΔG° is the reaction free (Gibbs) energy. The latter is given, however, with a positive sign due to the vertical uphill transition from the ground state to the exciplex. E_v is the energy of the donor−acceptor vibrational mode, M is the transition dipole moment, k_B is Boltzmann constant, h is the Planck constant, and n is the refractive index of the solvent. Applying these equations we fitted the emission spectra of the dyads. Representative fitting curves are given in Figure 4 as solid lines, whereas the experimental data are depicted as dots. In general, the fitted curves follow well the experimental data throughout the spectral region, with the exception of the shoulder in the blue region. We wish to reiterate that the blue emission relates to the residual porphyrin fluorescence, which remains appreciable in this region.

The fitting procedure allows one to obtain reliable values for λ_s, λ_v, E_v, ΔG°, and C_e. The coefficient C_e is a frequency independent scaling factor and determines only the emission density. Since the absolute value of the emission density was unavailable for our experiments, we conclude that the calculated value of C_e bears no physical meaning and will not be discussed in the current context. Conversely, the remaining four parameters, λ_s, λ_v, E_v, and ΔG°, characterize the energetics of the exciplex state. The results of the fits are summarized in Table 1 for all the compounds studied. As expected the exciplex is characterized by a rather low reorganization energy, λ_s, which is in good agreement with the values reported previously for compact single linked dyads.[4,6]

Our instruments allowed us to record the entire emission spectra of the **H₂P** dyads, while for the **ZnP** dyads, and
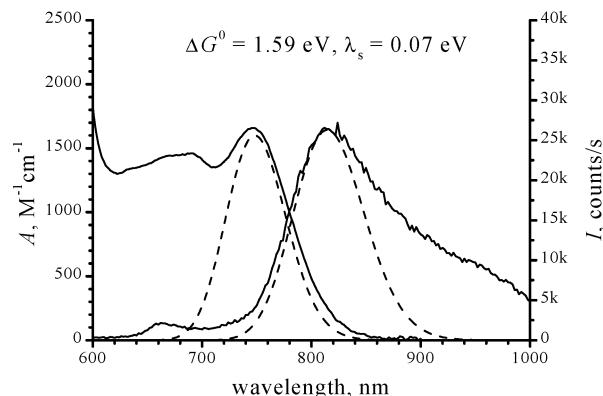
Figure 5. Absorption and emission spectra of **ZnTBD6be** in cyclohexane in the near-infrared region (solid lines) together with the model curves (dashed lines) calculated by eqs 3 and 4, using common values of ΔG° and λ_s.

TABLE 1: CT Parameters (ΔG°, λ_s, λ_v, E_v) Obtained from Steady State Emission Spectra

compd	solvent	ΔG°, eV	λ_s, eV	λ_v, eV	E_v, eV
DHD6ee	toluene	1.742	0.123	0.027	0.20
ZnDHD6ee	toluene	1.647	0.157	0.072	0.169
TBD6be	cyclohexane	1.74	0.06	0.03	0.14
	toluene	1.71	0.10	0.02	0.18
ZnTBD6be	cyclohexane	1.617	0.105	0.089	0.177
	toluene	1.589	0.108	0.137	0.150
TBD4be	toluene	1.736	0.129	0.034	0.201
ZnTBD4be	toluene	1.713	0.20	0.16	0.215
ZnD7me	toluene	1.64 (fixed)	0.126	0.19	0.173

especially in solvents more polar than cyclohexane, the red shoulder of the emission band falls outside of the detectable range. In addition, the instrumental correction of the emission spectra at wavelengths >950 nm is unreliable. Thus the fits obtained for the **ZnP** dyads are less accurate compared to those carried out for the **H₂P** dyads.

The near-infrared part of the absorption and the emission spectra of **ZnTBD6be** in cyclohexane are presented in Figure 5. Since absorption and emission are both transitions between the same electronic states, we treated them using the Marcus theory again.[23] The absorbance is given by an equation similar to eq 1:

$$A(v) = C_a\sum_{i=0}^{\infty}\frac{S^n}{i!}\exp\left[-\frac{(hv - \Delta G^\circ - \lambda_s - iE_v)^2}{4\lambda_s kT}\right] \quad (2)$$

where again C_a is a frequency independent coefficient,[24] and ΔG° is the reaction free energy. To keep the same notations for both the absorption and the emission, the absorption transition free energy was selected as the measure of the energy difference between the ground state and the exciplex. Therefore, in the case of the emission, the free energy is $-\Delta G^\circ$, as it was used in eq 1.

The absorption spectra of the dyads consist, in the region of interest, of partially overlapping delocalized CT, localized porphyrin, and localized fullerene features. Unfortunately, the interchromophore interaction perturbs the initial porphyrin spectrum significantly and simply subtracting the spectra of porphyrin **THP** or **ZnTHP** and fullerene **D4Fee** references from the spectra of the dyads causes unwarranted results. This leads us to conclude that eq 2 is inappropriate to treat the absorption spectra in a manner equivalent to the fitting of the emission spectra (see eq 1). A realistic approach implies that for the porphyrin/fullerene dyads the parameter $S < 1$ and the major

Tuning Porphyrin−Fullerene π-Stacks

J. Phys. Chem. B, Vol. 108, No. 42, 2004 **16381**

components of the emission and absorption spectra originate from the transitions between states of zero vibrational levels, i.e., $i = 0$. Thus, a reasonable approximation for the emission and absorption spectra can be obtained from the following equations:

$$I_0(v) = C_e \exp\left[-\frac{(hv - \Delta G^\circ + \lambda_s)^2}{4\lambda_s kT}\right] \quad (3)$$

$$A_0(v) = C_a \exp\left[-\frac{(hv - \Delta G^\circ - \lambda_s)^2}{4\lambda_s kT}\right] \quad (4)$$

In accordance with eqs 3 and 4 the emission and absorption maxima are given as $v_{max}^e = (\Delta G^\circ - \lambda_s)/h$ and $v_{max}^a = (\Delta G^\circ + \lambda_s)/h$, respectively. Since the spectroscopic maxima are readily available from the emission and absorption spectra, the values for ΔG° and λ_s are obtained straightforward:

$$\Delta G^\circ = (v_{max}^a + v_{max}^e)h/2 \quad (5)$$

$$\lambda_s = (v_{max}^a - v_{max}^e)h/2 \quad (6)$$

Equations 5 and 6 are well-known relations. By using the ΔG° and λ_s values obtained, the absorption and emission of the samples can now be modeled. Typical results of such calculations are depicted as dashed lines in Figure 5. As expected, applying eq 3 leads to a reasonable good fit for the center and the blue region of the emission spectrum. The red region, on the other hand, which corresponds to vertical transitions to higher vibrational modes ($i = 1, 2, ...$), reveals a significant deviation between the model curve and the measured spectrum.

From the absorption spectra an opposite picture emerges, since the higher modes (i.e., transitions to vibrational levels with $i > 0$) govern the blue part of the band. Therefore, eq 4 models well the center region and the red shoulder of the spectrum. In summary, both spectra were modeled by using common values for ΔG° and λ_s, and a reasonably good agreement between the model (eqs 3 and 4) and the experimental data is achieved.

The model can also be used for a quantitative analysis of the exciplex. For known CT absorption features with a donor−acceptor center-to-center distance, R_{cc}, the electronic coupling matrix element, V, can be estimated with use of the following equation:[25]

$$V = \frac{2.06 \times 10^{-2}}{R_{cc}}\sqrt{\epsilon_{max}v_{max}\Delta v} \quad (7)$$

where ϵ_{max} is the molar absorptivity (M^{-1} cm^{-1}), v_{max} is the light frequency at the emission intensity maximum (cm^{-1}), and Δv is the bandwidth of the CT absorption (cm^{-1}). The values ϵ_{max}, v_{max}, and Δv can be extracted from the experimental data (ϵ_{max}) and the model absorption curve (v_{max} and Δv).[26] For **ZnTBD6be** one obtains $\epsilon_{max} \approx 1\ 300\ M^{-1}\ cm^{-1}$, $v_{max} \approx 13\ 400$ cm^{-1}, and $\Delta v \approx 1\ 360\ cm^{-1}$. Since the fullerene diameter is known (i.e. $\approx$7 Å) and the porphyrin−fullerene edge-to-edge distance is basically equivalent to the fullerene−porphyrin van der Waals contact (i.e. 3−4 Å), we assume the value of $R_{cc} \approx$ 7 Å to be reasonable estimation for all dyads. Thus, V is $\sim$450 cm^{-1} or 0.056 eV. This value indicates stronger coupling as compared to $V = 270\ cm^{-1}$ obtained for the compact porphyrin−fullerene dyads with one linker.[4] The electronic coupling is the important characteristic in the inter- and intramolecular electron transfer. For widely studied porphyrin−quinone dyads
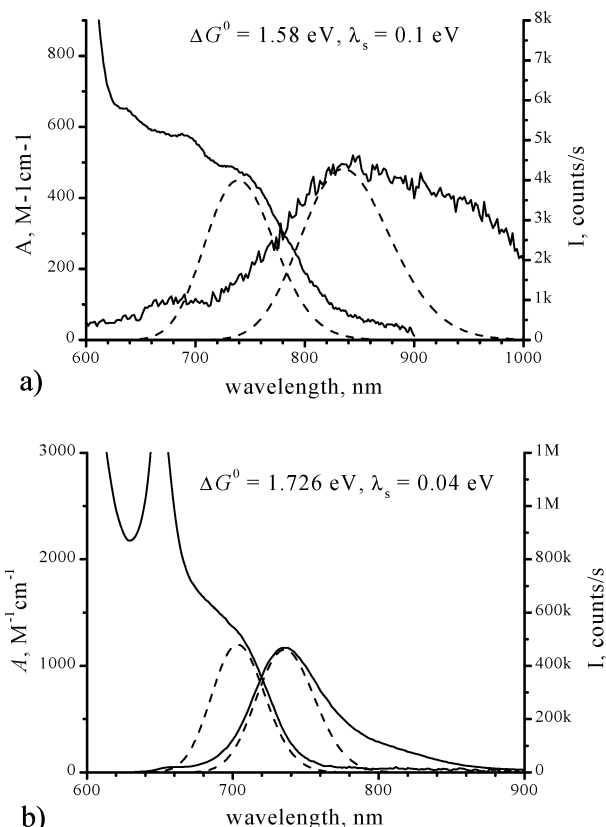
Figure 6. Absorption and emission spectra in the near-infrared region (solid lines) together with the model curves (dashed lines) calculated by eqs 3 and 4, using common values of ΔG° and λ_s: (a) **ZnD7me** in toluene and (b) **TBD6be** in cyclohexane.

a typical value of electronic coupling is a few units (in cm^{-1}). However, for similar double-linked porphyrin−quinone cyclophanes the electronic coupling was estimated to be as high as $140\ cm^{-1}$.[27]

Following the same approach we analyzed the remaining porphyrin/fullerene dyads. Examples of the fits are presented in Figures 5 and 6, and summarized in Table 2. Interestingly, the calculated V values reflect an eminent trend, namely, that the infrared absorption of the **ZnD7me** dyad is much lower in intensity than that of **ZnTBD6be**. This suggests that the electronic coupling for **ZnD7me** is lower than that of **ZnTBD6be**, which is in agreement with the calculated values.

In the case of the **H₂P** dyads, two trends emerge: (i) the exciplex state has a higher energy and (ii) the locally singlet excited state of the porphyrin has a lower energy relative to the ground state. Consequently, we noticed stronger overlapping features in the corresponding bands, which render this analysis method less reliable than that for the **ZnP** dyads. Still the ΔG° and λ_s values agree well with those derived from fitting the emission spectra and, thus, confirm the general applicability of this method even in the case of the **H₂P** dyads.

Formally, in the case of the **H₂P** dyads the fits of the emission spectra (eq 1, Figure 4) provide better estimations for the exciplex energetic compared to that obtained from the absorption−emission fits based on eqs 3 and 4 (Figure 5). In the case of the **ZnP** dyads the latter is the more accurate method. The difference arises from the fact that for the **H₂P** dyads the limiting factor is the absorption overlap between the chromophores and CT bands, while for the **ZnP** dyads the limiting factor is the incomplete and inaccurate measurements of the CT emission

TABLE 2: Common Analysis of the Absorption and Emission Spectra, Using Eqs 3 and 4

compd	solvent	ϵ_{max}, M^{-1} cm^{-1}	ν_{max}, cm^{-1}	$\Delta\nu$, cm^{-1}	V, cm^{-1} (meV)	$\Delta G°$, eV	λ_s, eV
DHD6ee	toluene	800	14450	1200	350 (43)	1.715	0.08
ZnDHD6ee	toluene	900	13600	1370	380 (47)	1.59	0.10
TBD6be	cyclohexane	1200	14230	850	350 (43)	1.726	0.04
	toluene	1000	14220	1170	380 (47)	1.692	0.075
ZnTBD6be	toluene	1300	13400	1360	450 (56)	1.56	0.10
	cyclohexane	1500	13400	1200	460 (57)	1.59	0.07
TBD4be	toluene	260	12250	1180	180 (22)	1.695	0.075
ZnTBD4be	toluene	190	14100	1490	190 (23)	1.63	0.12
ZnD7me	toluene	450	13500	1370	270 (33)	1.58	0.10

bands of their red parts. The calculated results obtained by these two methods are in good quantitative agreement for both types of dyads.

In the following we wish to compare three pairs of dyads as they bear linkers of different length: **ZnDHD6ee** vs **ZnD7me**, **ZnTBD6be** vs **ZnTBD4be**, and **TBD6be** vs **TBD4be**. For all pairs the values of $\Delta G°$ and λ_s are virtually the same. A sensible difference is, however, the electronic coupling, V. In principle, the highest values were obtained for the dyads with the dioxyethyl linkers (**ZnDHD6ee**, **ZnTBD6be**). Experimentally this is manifested in higher intensities of the CT band—compare, for example, Figures 5 and 6a. Another experimentally observed consequence of the higher electronic coupling is the higher exciplex emission intensity for the dioxyethyl-linked dyads. This can be rationalized on the basis of the following model:[21]

$$M = V\mu_{cp}/(h\nu_f)_{max} \qquad (8)$$

where μ_{cp} is the static dipole moment. The transition dipole moment can be used to express the electronic coupling, if μ_{cp} is assumed to be the same for all the dyads. In the case of the **ZnDHD6ee** and **ZnD7me** pair the result is obvious, as the **ZnD7me** dyad carries a longer linker and one can expect weaker interchromophore interaction. On the contrary, in the other pairs those dyads that bear a shorter linker (i.e., **TBD4be** and **ZnTBD4be**) give rise to lower electronic coupling. A possible rationale for this observation implies the structure of the oxymethyl linker. Oxymethyl linkers are short and thus fail to provide the necessary degree of freedom to allow the proper placement of the porphyrins on top of the 6:6 ring junction of the fullerene.[10]

We would like to finish this section by referring to another interesting experimental fact: the exciplex emission intensity is more than 10 times lower for the **ZnP** dyads relative to the **H₂P** dyads. The **ZnP** dyads reveal slightly higher electronic coupling, V, and stronger CT absorption intensity (see Table 2). Thus, from a pure theoretical consideration, as summarized in eq 1, it is feasible to anticipate stronger emission for the **ZnP** dyads, which is, however, not supported by the experiments, meaning that nonradiative relaxation of the exciplex is more efficient in the case of the **ZnP** dyads.

3.3. Photodynamics. The time-resolved spectroscopy experiments did confirm the expected functioning mechanism, and the quantitative values of rate constants were calculated. The experimental results were interpreted in the frame of the model previously[3b] applied to porphyrin−fullerene dyads with short separation.

3.3.1. Porphyrin Locally Excited State. The photodynamics of the excitation relaxation was studied with the pump−probe and the up-conversion techniques. The excitation wavelengths were 420−430 nm, which should populate the porphyrin second excited singlet state. For the **H₂P** systems the second excited state relaxes[28] to the first excited singlet state via internal conversion in a time scale less than 100 fs—faster than our instrumental response time. In other words, the first excited
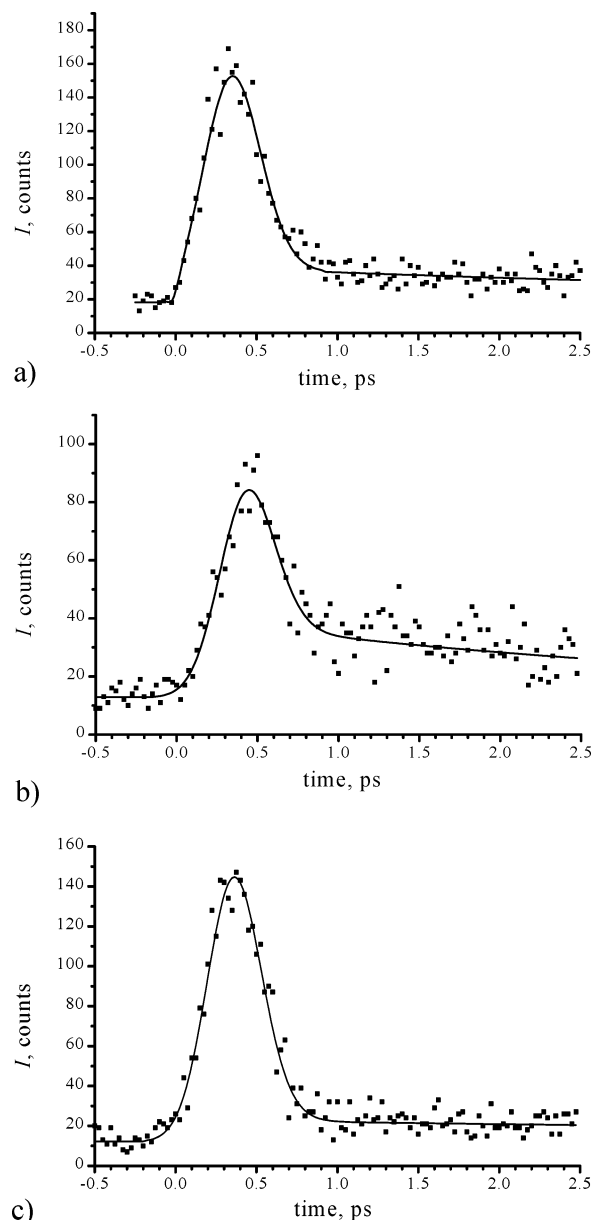

a)

b)

c)

Figure 7. Fluorescence decays of (a) **ZnD7me** in toluene, (b) **ZnD7me** in benzonitrile, and (c) **DHD6ee** in benzonitrile. The fast decay lifetimes are ca. 150 fs, and the emission wavelengths are 600 and 650 nm for **ZnD7me** and **DHD6ee**, respectively.

singlet state is the first detectable transient state. The best method to study dynamics of the excited singlet state is to measure the emission time profiles at 650−680 nm, which corresponds to the **H₂P** fluorescence. For all dyads and in all solvents the only detectable signal at this wavelength is a fast decay with a time constant approaching the time resolution limit of the instrument (Figure 7).[29]
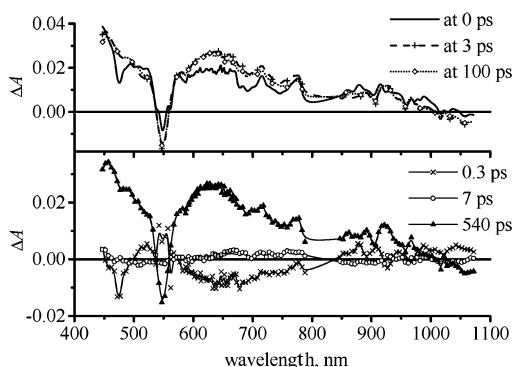
Figure 8. Transient absorption component spectra (bottom) and calculated time-resolved spectra (top) of **ZnTBD6be** in cyclohexane. The original pump−probe data were fitted with a 3-exponential model, and the lifetimes (bottom) and delay times (top) are indicated in the plot.

In the case of **ZnP**, the internal conversion is as slow as 1 ps.[28] In fact, typically this process is observed either as a decay at the red side of the Soret band at 450−500 nm or as a formation of the fluorescence at 590−660 nm. In our experiments the only detectable signal was the fast emission relaxation in the 590−660-nm range (Figure 7). The fluorescence relaxation was virtually the same for all dyads and in all solvents, with extremely low signal intensities. This suggests an additional, second relaxation pathway for the second excited state, competing efficiently with the internal conversion process. Regardless of the above-mentioned spectroscopic and kinetic characteristics, the locally excited singlet states of porphyrins relax extremely fast ($\tau < 200$ fs) to another intermediate state. It has previously been shown that in related porphyrin/fullerene dyads[2] the nature of this state is an intramolecular exciplex. We reach the same conclusion for the currently probed dyads, as is independently confirmed by the transient absorption measurements (vide infra) and by the strong exciplex emission detected for all the compounds in nonpolar solvents.

3.3.2. Exciplex in Nonpolar Solvents. The transient absorption was studied with the pump−probe technique. In Figure 8 the bottom plot shows spectra of the preexponential factors (or decay component spectra) obtained as a result of the global data fitting. The top plot presents time-resolved differential spectra calculated from the component spectra (bottom plot). The calculations are needed to compensate group velocity dispersion, which is essential at picosecond delay time. The longest available delay time of the instrument is 1.5 ns. In this time scale we observe a gradual relaxation of the transient absorption for the **ZnP** dyads, but for the **H₂P** dyads, in nonpolar solvents, the signal lifetimes were comparable or longer than the time scale of the measurements. Basically, the transient absorptions in nonpolar solvents consisted of a fast, nearly unresolved formation of the signal, and a relatively long-lived relaxation. An example of this kinetics is presented in Figure 9 for **ZnTBD6be** in cyclohexane. Although the data were best fitted by using a 3-exponential model the component, for which we determined a lifetime of 7 ps, is very weak in intensity in the recorded wavelength region. The fast relaxation of the porphyrin singlet excited state (200 fs) was only observed as a minor formation (e.g. at 675 nm, Figure 9) or decay component (e.g. 560 nm, Figure 9). The strongest time-resolved process is the relaxation of the signal with a time constant of 540 ps.

The nature of the exciplex gives rise to a strong emission, whose decay can be conveniently followed in the near-infrared region. The method of choice for performing these measurements was the time-correlated single-photon counting, which
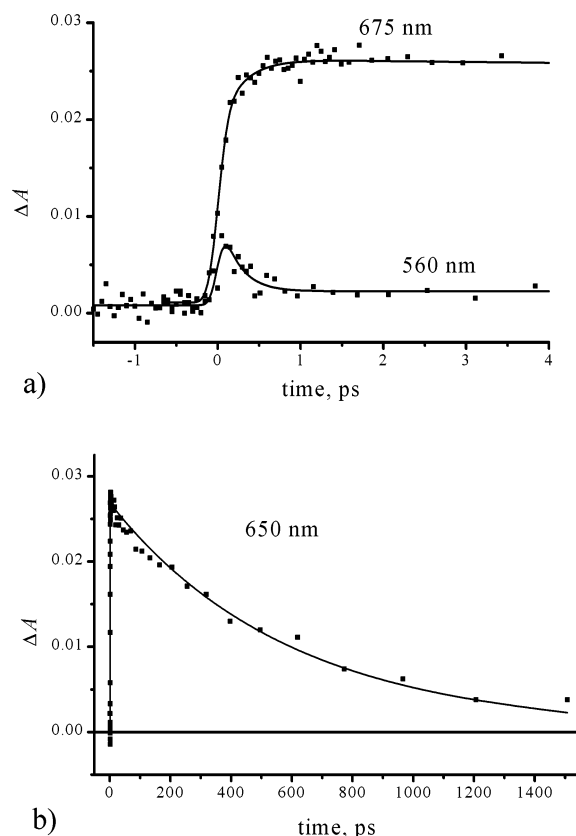

Figure 9. Transient absorption of **ZnTBD6be** in cyclohexane at selected wavelengths.
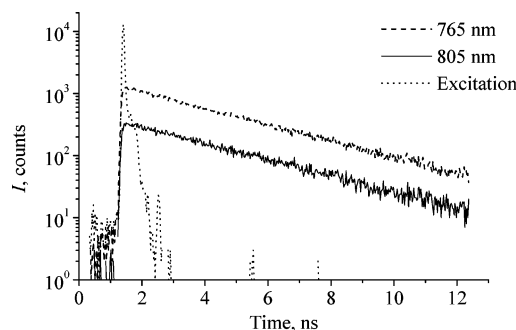
Figure 10. Time-correlated single-photon counting decays of TBD6be in toluene at two wavelengths. The excitation pulse profile is shown for reference.

revealed virtually the same lifetimes as the longest lived components in the pump−probe experiments. An example of experimental results for **TBD6be** in toluene is presented in the Figure 10. We ascribe the transient state, which is formed within a few hundreds of femtoseconds (after the initial excitation), as the intramolecular exciplex. At least for the **ZnP** dyads, the intramolecular exciplex relaxes to the ground state in a time scale of a few hundred picoseconds. Equation 9 summarizes the main excitation relaxation pathways:[30]

$$PC + h\nu \rightarrow P^{**}C \rightarrow P^*C \xrightarrow{k_{px}} (PC)^* \xrightarrow{k_{xg}} PC \qquad (9)$$
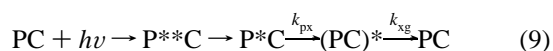
The rate constants of the reactions are summarized in Table 3. The values of the third column ($k_{px} + k_{pf}$) were obtained from the up-conversion measurements (inverse lifetime of the fast component), the fourth column (k_{fx}) from the pump−probe (inverse lifetime of the slow component), and the fifth column (k_{xg}) from the TCSPC experiments (inverse lifetime of the exciplex emission).

16384 *J. Phys. Chem. B, Vol. 108, No. 42, 2004*

Chukharev et al.

TABLE 3: Rate Constants for Compounds in Nonpolar Solvents

compd	solvent	$k_{pf} + k_{px}$,[a] s^{-1}	k_{fx},[b] s^{-1}	k_{xg},[c] s^{-1}
DHD6ee	toluene	6×10^{12}	71×10^9	0.34×10^9
ZnDHD6ee	toluene	10×10^{12}	29×10^9	2.4×10^9
TBD6be	toluene	6×10^{12}	83×10^9	0.31×10^9
ZnTBD6be	toluene	10×10^{12}	190×10^9	3.3×10^9
TBD4be	toluene	9×10^{12}	50×10^9	0.29×10^9
ZnTBD4be	toluene	9×10^{12}		2.0×10^9
ZnD7me	toluene	6×10^{12}	56×10^9	2.9×10^9
TBD6be	cyclohexane	10×10^{12}	*d*	0.36×10^9
ZnTBD6be	cyclohexane	10×10^{12}	*d*	1.6×10^9
TBD4be	cyclohexane	10×10^{12}	*d*	0.37×10^9

[a] $k_{pf} + k_{px}$ is the relaxation rate of the first singlet excited state, which is determined by two reactions: intramolecular energy transfer to the fullerene moiety and formation of the exciplex. [b] k_{fx} is the relaxation rate of the fullerene excited state to the exciplex. [c] k_{xg} is the relaxation rate of the exciplex. [d] Reliable value was not obtained.

a)

b)
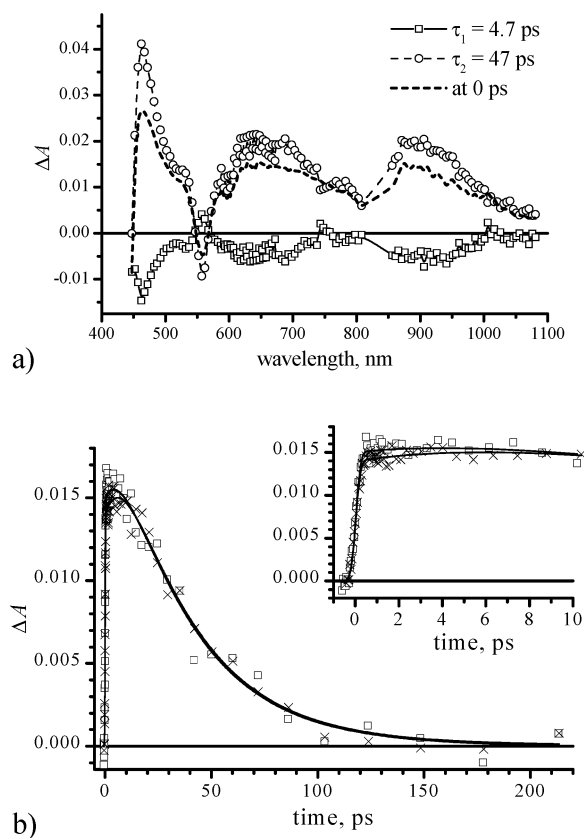
Figure 11. Transient absorption of **ZnD7me** in benzonitrile: (a) decay component spectra and calculated spectrum at zero delay time and (b) decay profiles at 650 (squares) and 900 nm (×); the solid lines show fitted curves.

3.3.3. Exciplex and Charge Separation in Benzonitrile. In benzonitrile no exciplex emission was observed. This implies that the exciplex emission is quenched more than 100 times compared to that in the nonpolar solvents. Therefore, the exciplex, if formed at all, should have a lifetime 100 times shorter than that in a nonpolar environment. However, the pump−probe measurements reveal transient states with lifetimes only ~10 times shorter than those in toluene. In addition to these intermediate states, which are characterized by relatively long lifetimes, picosecond transients are discernible showing the formation of new transient absorption bands at 650 and 900 nm. As an example the decay component spectra and the absorption time profiles are presented for **ZnD7me** in Figure 11. The component corresponding to the growth, which has a lifetime of ca. 5 ps, is relatively weak. In fact, it rather looks

**TABLE 4: Rate Constants for Compounds in Polar Solvent (bezonitrile)**

compd	k_{px},[a] s^{-1}	k_{xi}, s^{-1}	k_{ig}, s^{-1}
DHD6ee	1.0×10^{13}	1.0×10^{11}	2.6×10^9
ZnDHD6ee	2.3×10^{13}	7.7×10^{11}	1.6×10^{10}
TBD6be	8.3×10^{12}	1.5×10^{11}	2.2×10^9
ZnTBD6be	1.5×10^{13}	1.4×10^{12}	2.0×10^{10}
TBD4be	2.2×10^{13}	1.5×10^{11}	1.6×10^9
ZnD7me	1.1×10^{13}	1.8×10^{11}	2.3×10^{10}

[a] k_{px} is the relaxation rate of the first singlet excited state to the exciplex. [b] k_{xi} is the relaxation rate of the exciplex to the CS state. [c] k_{ig} is the relaxation rate of the CS state.

like a plateau instead of a real increase in the sample absorbance. It is also interesting to note that the time profiles of the signals at 650 and 900 nm are virtually identical.

A spectral comparison leads to the following assignment: we attribute the 900-nm absorption to the fullerene radical anion, while that at 650 nm bears close resemblance to the porphyrin radical cation. On the basis of this mechanistic picture, the process, for which we determined a time constant of 5 ps, is likely the formation of the charge separated state, whose formation was hampered in nonpolar solvents. The only reasonable candidate for the CS state precursor is the exciplex, as the porphyrin excited singlet state relaxes within a few hundred femtoseconds, according to the up-conversion measurements. Another possible candidate for the spectrum of the precursor, that is, the fullerene excited singlet state, can be ruled out, since the transient features a broad absorption band in the 600−700-nm region, unlike fullerene excited singlet states, whose most dominant transition is centered around 880−900 nm.

Considering all these observations the following reaction scheme emerges in the case of benzonitrile:

$$PC + h\nu \rightarrow P^{**}C \rightarrow P^*C \xrightarrow{k_{px}} (PC)^* \xrightarrow{k_{xi}} P^+C^- \xrightarrow{k_{ig}} PC \quad (10)$$
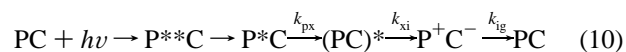
It should be noted that similar results were concluded from the time-resolved experiments performed with the other dyads. All the reaction rates are collected in Table 4. The values of the second column (k_{px}) were obtained from the up-conversion measurements (inverse lifetime of the fast component), while the third and the fourth columns (k_{xi} and k_{xg}) are from the pump−probe experiments (inverse lifetimes of the two components).

3.4. Comparison of the Reaction Rates. We estimate the quantum yield of the exciplex emission in nonpolar media to be roughly 1%.[31] This means that the emission of light is not the main path of the exciplex relaxation. From the known set of parameters λ_s, λ_v, E_v, $\Delta G°$, and V we can estimate the rate constant of nonradiative transition from the exciplex to the ground state.[21,23,32] The calculations give a value of $k_{xg} \approx 6 \times 10^5$ s^{-1} for **ZnDHD6ee**, which differs by many orders of magnitude from the experimental value, 2.4×10^9 s^{-1}. The theoretical models predict also that the rate is proportional to the square of the electronic coupling. In other words, for **TBD6be** the nonradiative relaxation rate is expected to be 4 times faster than that for **TBD4be**, but they are nearly the same, respectively 0.31×10^9 and 0.29×10^9 s^{-1}. This discrepancy implies that the relaxation from exciplex to the ground state proceeds via an additional intermediate state. The reasonable candidate for this intermediate state is the CS state. Suppose in nonpolar solvents the CS state is formed from exciplex and decays to the ground state faster than it is formed. Then we cannot observe the CS state in the pump−probe experiment because of too low population of the state. From comparison of the last columns of Tables 3 and 4 we can find that even if

Tuning Porphyrin−Fullerene π-Stacks

J. Phys. Chem. B, Vol. 108, No. 42, 2004 **16385**

the CS state in nonpolar solvent decays 10 times slower than in polar solvents, one cannot detect the CS state in pump−probe experiments with nonpolar solvents.

The hypothesis of exciplex relaxation via an additional (supposedly CS) state in nonpolar solvents can simplify the explanation of the fact that dyads with **ZnP** have about a 10 times shorter lifetime of exciplex decay than **H2P** dyads. For two states with close energies even a small change in the energy level of one state leads to a big change of the rate constant for the transition between the states. Indeed, the most important difference between the **H₂P** and **ZnP** dyads is the energy of the exciplex, $\Delta G°$, whereas all the other parameters, λ_s, λ_v, E_v, and V, are virtually identical. According to eq 1 this gives roughly the same emission rates, in agreement with experiment. Note also that in polar solvent the CS state decays approximately 10 times faster for **ZnP** dyads than for **H₂P** dyads.

4. Conclusion

A set of porphyrin−fullerene dyads with two separate linkers was studied by time-resolved and steady state spectroscopic methods. The dyads feature an unprecedentedly high CT absorption band. The analysis of steady-state spectra in the frame of the Marcus electron transfer theory shows that the electronic coupling matrix element V is highest for the dioxyethyl type of linkers and smaller for the shorter and the longer linkers. We propose a hypothesis that in nonpolar solvents the exciplex relaxation goes via an intermediate state, supposedly the CS state, which decays faster than it is formed. This hypothesis comes from the comparison of theory predicted rate constants with the results of time-resolved spectroscopy.

References and Notes

(1) (a) Tkachenko, N. V.; Rantala, L.; Tauber, A. Y.; Helaja, J.; Hynninen, P. H.; Lemmetyinen, H. *J. Am. Chem. Soc.* **1999**, *121*, 9378−9387. (b) Vehmanen, V.; Tkachenko, N. V.; Tauber, A. Y.; Hynninen, P. H.; Lemmetyinen, H. *Chem. Phys. Lett.* **2001**, *345*, 213−218.

(2) Kesti, T. J.; Tkachenko, N. V.; Vehmanen, V.; Yamada, H.; Imahori, H.; Fukuzumi, S.; Lemmetyinen, H. *J. Am. Chem. Soc.* **2002**, *124*, 8067−8077.

(3) (a) Vehmanen, V.; Tkachenko, N. V.; Efimov, A.; Damlin, P.; Ivaska, A.; Lemmetyinen, H. *J. Phys. Chem. A* **2002**, *106*, 8029−8038. (b) Tkachenko, N. V.; Lemmetyinen, H.; Sonoda, J.; Ohkubo, K.; Sato, T.; Imahori, H.; Fukuzumi, S. *J. Phys. Chem. A* **2003**, *107*, 8834−8844.

(4) Imahori, H.; Tkachenko, N. V.; Vehmanen, V.; Tamaki, K.; Lemmetyinen, H.; Sakata, Y.; Fukuzumi, S. *J. Phys. Chem. A* **2001**, *105*, 1750−1756.

(5) Armaroli, N.; Marconi, G.; Echegoyen, L.; Bourgeois, J.-P.; Diederich, F. *Chem. Eur. J.* **2000**, *6* (9), 1629−1645.

(6) Vehmanen, V.; Tkachenko, N. V.; Imahori, H.; Fukuzumi, S.; Lemmetyinen, H. *Spectrochim. Acta A* **2001**, *57* (11), 2227−2242.

(7) Imahori, H.; Ozawa, S.; Ushida, K.; Takahashi, M.; Azuma, T.; Ajavakom, A.; Akiyama, T.; Hasegawa, M.; Taniguchi, S.; Okada, T.; Sakata, Y. *Bull. Chem. Soc. Jpn.* **1999**, *72*, 485−502.

(8) Tkachenko, N. V.; Guenther, C.; Imahori, H.; Tamaki, K.; Sakata, Y.; Fukuzumi, S.; Lemmetyinen, H. *Chem. Phys. Lett.* **2000**, *326*, 344−350.

(9) (a) Olmstead, M. M.; Costa, D. A.; Maitra, K.; Noll, B. C.; Phillips, S. L.; Van Calcar, P. M.; Balch, A. L. *J. Am. Chem. Soc.* **1999**, *121*, 7090−7097. (b) Boyd, P. D. W.; Hodgson, M. C.; Richard, C. E. F.; Oliver, A. G.; Chaker, L.; Brothers, P. J.; Bolskar, R. D.; Tham, F. S.; Reed, C. A. *J. Am. Chem. Soc.* **1999**, *121*, 10487−10495. (c) Evans, D. R.; Fackler, N. L. P.; Xie, Z.; Rickard, C. E. F.; Boyd, P. D. W.; Reed, C. A. *J. Am. Chem. Soc.* **1999**, *121*, 8466−8474.

(10) Sun, Y.; Drovetskaya, T.; Bolskar, R. D.; Bau, R.; Boyd, P. D. W.; Reed, C. A. *J. Org. Chem.* **1997**, *62*, 3642−3649.

(11) Sun, D.; Tham, F. S.; Reed, C. A.; Chaker, L.; Boyd, P. D. W. *J. Am. Chem. Soc.* **2002**, *124*, 6604−6612.

(12) Konarev, D. V.; Neretin, I. S.; Slovokhotov, Y. L.; Yudanova, E. I.; Drichko, N. V.; Shul'ga, Y. M.; Tarasov, B. P.; Gumanov, L. L.; Batsanov, A. S.; Howard J. A. K.; Lyubovskaya R. N. *Chem. Eur. J.* **2001**, *7*, 2605−2616.

(13) (a) Imahori, H.; Hagiwara, K.; Aoki, M.; Akiyama, T.; Taniguchi, S.; Okada, T.; Shirakawa, M.; Sakata, Y. *J. Am. Chem. Soc.* **1996**, *118*, 11771−11782. (b) Imahori, H.; Sakata, Y. *Adv. Mater.* **1997**, *9*, 537. (c) Imahori, H.; Mori, Y.; Matano, Y. *Photochem. Photobiol. C* **2003**, *4*, 51.

(14) (a) Kuciauskas, D.; Lin, S.; Seely, G. R.; Moore, A. L.; Moore; T. A.; Gust, D.; Drovetskaya, T.; Reed, C. A.; Boyd, P. D. W. *J. Phys. Chem.* **1996**, *100*, 15926−15932. (b) Gust, D.; Moore, T. A.; Moore, A. L. *Acc. Chem. Res.* **2001**, *34*, 40−48.

(15) (a) D'Souza F.; Gadde, S.; Zandler, M. E.; Arkady, K.; El-Khouly, M. E.; Fujitsuka, M.; Ito, O. *J. Phys. Chem. A* **2002**, *106*, 12393−12404. (b) D'Souza, F.; Deviprasad, G., R.; Zandler, M. E.; El-Khouly, M. E.; Fujitsuka, M.; Ito, O. *J. Phys. Chem. B* **2002,** *106*, 4952−4962.

(16) Dietel, E.; Hirsch, A.; Eicchorn, E.; Rieker, A.; Hackbarth, S.; Roder, B. *Chem. Commun.* **1998**, 1981.

(17) Guldi, D. M.; Luo, C.; Prato, M.; Troisi, A.; Zerbetto, F.; Scheloske, M.; Dietel, E.; Bauer, W.; Hirsch, A. *J. Am. Chem. Soc.* **2001**, *123*, 9166−9167.

(18) Efimov, A.; Vainiotalo, P.; Tkachenko, N. V.; Lemmetyinen, H. *J. Porphyrins Phthalocyanines* **2003**, *7:9*, 610.

(19) Schuster, D. I.; Cheng, P.; Wilson, S. R.; Prokhorenko, V.; Katterle, M.; Holzwarth, A. R.; Braslavsky, S. E.; Klihm, G.; Williams, R. M.; Luo, C. *J. Am. Chem. Soc.* **1999**, *121*, 11599−11600.

(20) Scheloske, M. Dissertation, Erlangen, 2003.

(21) (a) Gould, I. R.; Young, R. H.; Moody, R. E.; Farid, S. *J. Phys. Chem.* **1991**, *95*, 2068−2080. (b) Gould, I. R.; Young, R. H.; Mueller, L. J.; Farid, S. *J. Am. Chem. Soc.* **1994**, *116*, 8167−8187. (c) Gould, I. R.; Young, R. H.; Mueller, L. J.; Farid, S. *J. Am. Chem. Soc.* **1994**, *116*, 8188−8199. (d) Bixon, M.; Jortner, J.; Verhoeven, J. W. *J. Am. Chem. Soc.* **1994**, *116*, 7349−7355. (e) Katz, N. E.; Mecklenburg, S. L.; Graff, D. K.; Chen, P.; Meyer, T. J. *J. Phys. Chem.* **1994**, *98*, 8959−8961. (f) Liu, J.-Y.; Bolton, J. R. *J. Phys. Chem.* **1992**, *96*, 1718−1725.

(22) (a) Palmans, J. P.; Swinnen, A. M.; Desie, G.; Van Der Auweraer, M.; Vandendriessche, J.; De Schryver, F. C.; Mataga, N. *J. Photochem.* **1985**, *28*, 419−431. (b) Wasielewski, M. R.; Minsek, D. W.; Niemczyk, M. P.; Svec, W. A.; Yang, N. C. *J. Am. Chem. Soc.* **1990**, *112*, 2823−2824. (c) Verhoeven, J. W. *Pure Appl. Chem.* **1990**, *62*, 1585−1596. (d) Van der Auweraer, M.; Grabowski, Z. R.; Rettig, W. *J. Phys. Chem.* **1991**, *95*, 2083−2092. (e) Chow, Y. L.; Johansson, C. I. *J. Phys. Chem.* **1995**, *99*, 17558−17565. (f) Seshadri, R.; Rao, C. N. R.; Pal, H.; Mukherjee, T.; Mittal, J. P. *Chem. Phys. Lett.* **1993**, *205*, 395−398.

(23) Marcus, R. A. *J. Phys. Chem.* **1989**, *93*, 3078−3086.

(24) According to Marcus $C_a = (8\pi^3 N_A/3000hnc \; \ln 10)(|\mu_{rp}|^2 e^{-S}/Q_r)$.

(25) (a) Barbara, P. F.; Meyer, T. J.; Ratner, M. A. *J. Phys. Chem.* **1996**, *100*, 1348. (b) Chen, P.; Meyer, T. J. *Chem. Rev.* **1998**, *98*, 1439−1477.

(26) It is arguable what the accuracy is of the bandwidth estimation from the model curve given by eq 4. Figure 5 indicates that the real bandwidth can be 50% greater. However, the estimated bandwidths will be used for comparison of different dyads, for which one can assume the same correction factor.

(27) (a) Scherer, P. O. J.; Fischer, S. F. *Chem. Phys. Lett.* **1992**, *190*, 574−580. (b) Frey, W.; Klann, R.; Laermer, F.; Elsaesser, T. *Chem. Phys. Lett.* **1992**, *190*, 567−573. (c) Häberle, T.; Hirsch, J.; Pöllinger, F.; Heitele, H.; Michel-Beyerle, M. E.; Anders, C.; Döhling, A.; Krieger, C.; Rückemann, A.; Staab, H. A. *J. Phys. Chem.* **1996**, *100*, 18269−18274. (d) Tsue, H.; Imahori, H.; Kaneda, T.; Tanaka, Y.; Okada, T.; Tamaki, K.; Sakata, Y. *J. Am. Chem. Soc.* **2000**, *122*, 2279−2288. (e) Hayashi, S.; Kato, S. *J. Phys. Chem. A* **1998**, *102*, 2878−2887. (f) Sakata, Y.; Tsue, H.; O'Neil, M. P.; Wiederrecht, G. P.; Wasilewski, M. R. *J. Am. Chem. Soc.* **1994**, *116*, 6904−5909.

(28) Akimoto, S.; Yamazaki, T.; Yamazaki, I.; Osuka, A. *Chem. Phys. Lett.* **1999**, *309*, 177−182.

(29) The second possible component in Figure 7b has intensity less than 2 photons per second and is at the noise level. Porphyrin has hundreds of times more intense emission, therefore even 0.1% of porphyrin in the dyad could give this signal.

(30) At least for **ZnP** dyads one can consider an alternative formation pathway of the exciplex: ... → P*C (k_{pf}) → P*C (k_{fx}) → (PC)* → .... This process is probably observed as the mentioned minor component with a 7-ps lifetime in the case of **ZnTBD6be** in cyclohexane.

(31) No accurate measurements of the quantum yields were performed. Rough estimations were made relative to the porphyrin reference compound fluorescence, and have shown that the exciplex emission was not greater than 1/10 of that.

(32) Jortner, J.; Bixon, M. *J. Chem. Phys.* **1988**, *88* (1), 167−170.